АСТРОФИЗИКА

ТОМ 66 ФЕВРАЛЬ, 2023 ВЫПУСК 1

DOI: 10.54503/0571-7132-2023.66.1-95

EFFECT OF THE INTERACTION BETWEEN HYPERONS ON THE MOMENT OF INERTIA OF THE PROTO NEUTRON STARS

XIAN-FENG ZHAO

Received 12 October 2022
Accepted 3 February 2023

Effect of the interaction between hyperons on the moment of inertia of proto neutron stars (PNSs) PSR J0740+6620, PSR J0348+0432, PSR J1614-2230 and PSR J0737-3039A is examined by means of relativistic mean field theory. Taking into account the interaction between hyperons, the mass M of the PNS decreases with respect to the same radius R, the energy density ε increases with respect to the same pressure p, and the moment of inertia I of the PNS decreases with respect to the same central energy density ε_c. Under the constraint of the mass of the PNS, considering the interaction between hyperons, the larger the mass of the PNS, the more the radius and moment of inertia of the PNS decrease, while the more energy density and pressure increase. For smaller PNSs, the effect can be negligible.

Keywords: *hyperon: relativistic mean field theory: neutron star*

1. *Introduction.* Neutron stars (NSs) are dense objects that have a $\lesssim 2$ solar mass and a very small radius [1-4]. When calculating its moment of inertia, general relativistic effects must be taken into account [5,6].

A binary NS system PSR J0737-3039 was observed in 2004 [7]. One of the NSs in the system, NS PSR J0737-3039A, has a typical mass $M = 1.34 M_{\odot}$ [7-9]. After that, its mass was determined to be $M = 1.337 M_{\odot}$ [10], or $M = 1.3381 \pm 0.0007 M_{\odot}$ [11].

In the last decade, great progress has also been made in the observation of massive NSs. NS PSR J1614-2230 was discovered in 2010 and its mass is $M = 1.97 \pm 0.04 M_{\odot}$ [12]. In 2016, its mass was precisely determined to be $M = 1.93 \pm 0.07 M_{\odot}$ [13]. NS PSR J0348+0432, whose mass is $M = 2.01 \pm 0.04 M_{\odot}$, was observed in 2013 [14]. In 2020, NS PSR J0740+6620 with the mass of $M = 2.14^{+0.10}_{-0.09} M_{\odot}$ was discovered [15] and it may be the most massive NS ever discovered.

NSs come from supernova explosions. A proto neutron star (PNS), formed by a supernova explosion, can reach temperatures as high as 30 MeV. Later, the PNS emits energy through neutrino radiation to form a NS [16]. PNS is a very important stage in the evolution of NS and the research of PNS is meaningful for astrophysics.

The interactions between nucleons in NS matter are described by σ, ω and ρ mesons. But this is not complete, and the interactions between hyperons, which can be described in terms of f_0 (1020 MeV) (short for σ^*) and ϕ (975 MeV) (short for ϕ) mesons [17], need to be taken into account. It is of great interest to know how the interaction between hyperons affects the properties of the PNS, such as the moment of inertia.

In this paper, the effect of the interaction between hyperons on the moment of inertia of PNSs PSR J0740+6620, PSR J0348+0432, PSR J1614-2230 and PSR J0737-3039A is examined by using the relativistic mean field (RMF) theory [18] considering baryon octet.

2. *The RMF theory for the PNS matter*. The Lagrangian density of the PNS matter is as follows [19]

$$\begin{aligned}\mathcal{L} = &\sum_B \overline{\psi}_B\left(i\gamma_\mu\partial^\mu - m_B + g_{\sigma B}\,\sigma + g_{\sigma^* B}\,\sigma^* - g_{\omega B}\,\gamma^0\omega_0 - g_{\phi B}\,\gamma^0\phi_0 - g_{\rho B}\,\gamma^0\tau_3\rho_{03}\right)\psi_B \\ &-\frac{1}{2}m_\sigma^2\sigma^2 - \frac{1}{3}g_2\sigma^3 - \frac{1}{4}g_3\sigma^4 + \frac{1}{2}m_\omega^2\omega_0^2 + \frac{1}{2}m_\rho^2\rho_{03}^2 - \frac{1}{2}m_{\sigma^*}^2\sigma^{*2} + \frac{1}{2}m_\phi^2\phi_0^2 \\ &+ \sum_{\lambda=e,\mu}\overline{\psi}_\lambda\left(i\gamma_\mu\partial^\mu - m_\lambda\right)\psi_\lambda .\end{aligned} \tag{1}$$

where ψ_B is the Dirac spinor of baryon B and the corresponding mass is m_B. σ and σ^* are field operators for mesons σ and σ^*, respectively. ω_0, ρ_{03} and ϕ_0 are expected values for mesons ω, ρ and ϕ, respectively. $g_{\sigma B}$, $g_{\omega B}$, $g_{\rho B}$, $g_{\sigma^* B}$ and $g_{\phi B}$ represent the coupling constants between σ, ω, ρ, σ^* and ϕ mesons and baryon B, respectively. g_2 and g_3 are the self-interaction parameters of σ mesons. m_σ, m_ω, m_ρ, m_{σ^*} and m_ϕ are masses of mesons σ, ω, ρ, σ^* and ϕ, respectively. ψ_λ and m_λ are the Dirac spinor and mass of the free electron and μ, respectively.

Considering the neutrino binding, the baryonic partition function of the PNS matter is

$$\ln Z_B = \frac{V}{T}\langle\mathcal{L}\rangle + V\sum_B\frac{2J_B+1}{2\pi^2}\int_0^\infty k^2dk\left\{\ln\left[1+e^{-(\varepsilon_B(k)-\mu_B)/T}\right]\right\}. \tag{2}$$

Here, V stands for volume, T for temperature, J_B for spin of baryon B, k for Fermi momentum, $\varepsilon_B(k)$ for energy of baryon B, and μ_B for chemical potential of baryon B.

The total baryon number density [20,21] is

$$\rho = \sum_B\frac{2J_B+1}{2\pi^2}b_B\int_0^\infty k^2 n_B(k)dk\,. \tag{3}$$

Here, b_B is the baryon number of baryon B. $n_B(k)$ is the Fermi-Dirac distribution function of baryon

$$n_B(k) = \frac{1}{1+\exp[(\varepsilon_B(k)-\mu_B)/T]}, \tag{4}$$

and $\varepsilon_B(k)$ is defined as

$$\varepsilon_B(k) = \sqrt{(m_B - g_{\sigma B}\sigma - g_{\sigma^* B}\sigma^*)^2 + k^2} + g_{\omega B}\omega_0 + g_{\phi B}\phi_0 + g_{\rho B}\rho_{03} I_{3B}, \tag{5}$$

where the interaction terms between baryon and meson fields are properly taken into account [22]. I_{3B} is the isospin 3 component of baryon B.

The energy density and the pressure respectively are

$$\begin{aligned}\varepsilon_B &= \frac{1}{2}m_\sigma^2\sigma^2 + \frac{1}{2}m_{\sigma^*}^2\sigma^{*2} + \frac{1}{3}g_2\sigma^3 + \frac{1}{4}g_3\sigma^4 \\ &+ \frac{1}{2}m_\omega^2\omega_0^2 + \frac{1}{2}m_\phi^2\phi_0^2 + \frac{1}{2}m_\rho^2\rho_{03}^2 + \sum_B \frac{2J_B+1}{2\pi^2}\int_0^\infty \kappa^2 n_B(k)\, d\kappa \sqrt{\kappa^2 + m_B^{*2}},\end{aligned} \tag{6}$$

$$\begin{aligned}p_B &= -\frac{1}{2}m_\sigma^2\sigma^2 - \frac{1}{2}m_{\sigma^*}^2\sigma^{*2} - \frac{1}{3}g_2\sigma^3 - \frac{1}{4}g_3\sigma^4 \\ &+ \frac{1}{2}m_\omega^2\omega_0^2 + \frac{1}{2}m_\phi^2\phi_0^2 + \frac{1}{2}m_\rho^2\rho_{03}^2 + \frac{1}{3}\sum_B \frac{2J_B+1}{2\pi^2}\int_0^\infty \frac{\kappa^4}{\sqrt{\kappa^2+m_B^{*2}}} n_B(k)\, d\kappa.\end{aligned} \tag{7}$$

Here, m_B^* is the effective mass of baryon B

$$m_B^* = m_B - g_{\sigma B}\sigma - g_{\sigma^* B}\sigma^*. \tag{8}$$

Regardless of the interaction between leptons at finite temperature, their partition function is

$$\ln Z_L = \frac{V}{T}\sum_i \frac{\mu_i^4}{24\pi^2}\left[1 + 2\left(\frac{\pi T}{\mu_i}\right)^2 + \frac{7}{15}\left(\frac{\pi T}{\mu_i}\right)^4\right] + V\sum_\lambda \frac{1}{\pi^2}\int_0^\infty k^2 dk\left\{\ln\left[1 + e^{-(\varepsilon_\lambda(k)-\mu_\lambda)/T}\right]\right\}, \tag{9}$$

the first line represents the contribution of massless neutrinos and the second line the contribution of electrons and μs. μ_i is the chemical potential of neutrinos. $\varepsilon_\lambda(k)$ and μ_λ are the energy and chemical potential of electrons and μs, respectively.

The lepton number density is

$$\rho_l = \frac{1}{\pi^2}\int_0^\infty k^2 n_l(k)\, dk, \tag{10}$$

$$\rho_\nu = \frac{\pi^2 T^2 \mu_\nu + \mu_\nu^3}{6\pi^2}. \tag{11}$$

where, ρ_l and $n_l(k)$ represent the number density and distribution function of electron and μ, respectively. ρ_ν and μ_ν represent the number density and chemical potential of electron neutrinos and μ neutrinos, respectively.

The energy density and the pressure of leptons are

$$\varepsilon_L = \sum_l \frac{1}{\pi^2}\int_0^\infty \kappa^2 n_l(k) d\kappa \sqrt{\kappa^2 + m_l^2} + \sum_\nu \left(\frac{7\pi^2 T^4}{120} + \frac{T^2 \mu_\nu^2}{4} + \frac{\mu_\nu^4}{8\pi^2} \right), \tag{12}$$

$$p_L = \frac{1}{3}\sum_l \frac{1}{\pi^2}\int_0^\infty \frac{\kappa^4}{\sqrt{\kappa^2 + m_l^2}} n_l(k) d\kappa + \sum_\nu \frac{1}{360}\left(7\pi^2 T^4 + 30 T^2 \mu_\nu^2 + \frac{15\mu_\nu^4}{\pi^2} \right). \tag{13}$$

The chemical potentials of baryon i are

$$\mu_i = \mu_n - q_i(\mu_e - \mu_{\nu e}). \tag{14}$$

where μ_n, μ_e and $\mu_{\nu e}$ denote the chemical potential of neutrons, the chemical potential of electrons and the chemical potential of electron neutrinos, respectively. q_i is the charge of baryon i.

The mass and the radius of a PNS can be calculated by the Tolman-Oppenheimer-Volkoff (TOV) equation [23,24]

$$\frac{dp}{dr} = -\frac{(p+\varepsilon)(M + 4\pi r^3 p)}{r(r-2M)}, \tag{15}$$

$$M = 4\pi\int_0^R \varepsilon r^2 dr. \tag{16}$$

For a slowly rotating PNS, its moment of inertia is [5,6]

$$I = \frac{8\pi}{3}\int_0^R dr r^4 \frac{\varepsilon + p}{\sqrt{1-2M(r)/r}} \frac{[\Omega - \omega(r)]}{\Omega} e^{-\nu}. \tag{17}$$

Here, Ω and $\omega(r)$ represent the angular velocity measured at infinity and the angular velocity of the frame rotation, respectively. ν is given by

$$-\frac{d\nu(r)}{dr} = \frac{1}{\varepsilon + p}\frac{dp}{dr}, \tag{18}$$

and the angular velocity is given by

$$-\frac{1}{r^4}\frac{d}{dr}\left(r^4 j \frac{d\bar{\omega}}{dr} \right) + \frac{4}{r}\frac{dj}{dr}\bar{\omega} = 0. \tag{19}$$

The $j(r)$ is

$$j(r) = e^{-(\nu+\lambda)} = e^{-\nu}\sqrt{1-2M(r)/r}, \quad r < R. \tag{20}$$

The boundary condition are given by

$$\frac{d\bar{\omega}}{dr}_{|r=0} = 0, \tag{21}$$

$$\nu(\infty)=0, \tag{22}$$

$$\overline{\omega}(R)=\Omega-\frac{R}{3}\frac{d\overline{\omega}}{dr}_{|r=R}. \tag{23}$$

3. *The parameters*. Eight sets of nucleon coupling constants (DD-MEI [25], FSU2H [26], FSU2R [26], FSUGold [27], GL85 [28], GL97 [19], GM1 [29], and TW99 [25]) are used to calculate the PNSs in this work.

The ratios of hyperon coupling constant to nucleon coupling constant can be defined as $x_{\sigma h}=g_{\sigma h}/g_{\sigma}$, $x_{\omega h}=g_{\omega h}/g_{\omega}$, $x_{\rho h}=g_{\rho h}/g_{\rho}$, with h denoting hyperons Λ, Σ and Ξ.

Through quark SU(6) symmetry we select the $x_{\rho h}s$ [30,31]. For the mass of the PNS increases as $x_{\sigma h}s$ and $x_{\omega h}s$ increase [32] and in order to obtain the large mass of the PNS PSR J0740+6620, we should select as large $x_{\omega h}s$ as possible, $x_{\omega h}=0.9$, and $x_{\sigma h}s$ are obtained by [19]

$$U_h^{(N)}=m_n\left(\frac{m_n^*}{m_n}-1\right)x_{\sigma h}+\left(\frac{g_\omega}{m_\omega}\right)^2\rho_0\,x_{\omega h}. \tag{24}$$

Here, the hyperon-potentials are chosen as $U_\Lambda^{(N)}=-30$ MeV [31,33,34], $U_\Sigma^{(N)}=30$ MeV [31,33-35] and $U_\Xi^{(N)}=-14$ MeV [36], respectively.

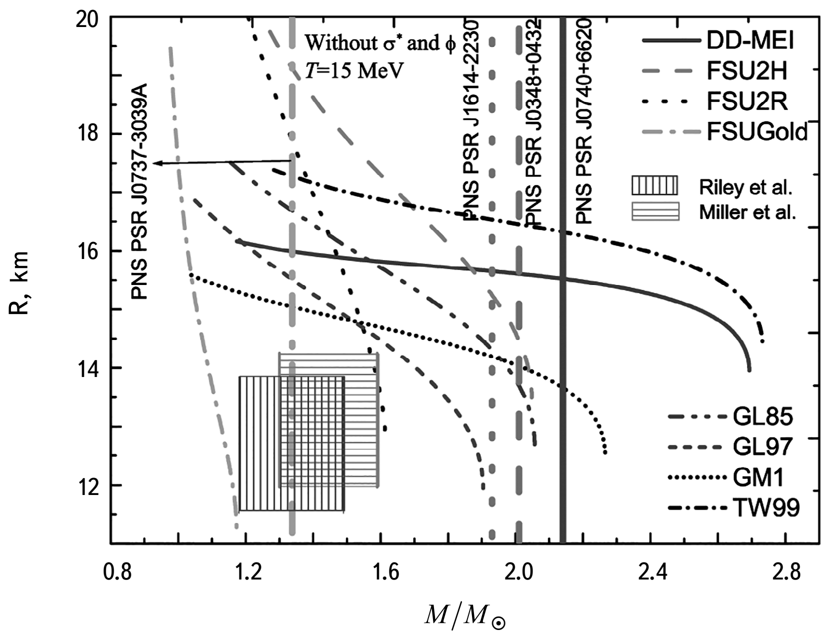

Fig.1. The radius of the PNS as a function of the mass. The four thick vertical lines represent the masses of the PNSs PSR J0740+6620, PSR J0348+0432, PSR J1614-2230 and PSR J0737-3039A, respectively.

The coupling parameters between the mesons σ^* and ϕ and the hyperons can be taken as [17]

$$g_{\phi\Xi} = 2g_{\phi\Lambda} = 2g_{\phi\Sigma} = -2\sqrt{2}\,g_\omega/3, \tag{25}$$

$$g_{\sigma^*\Lambda}/g_\sigma = g_{\sigma^*\Sigma}/g_\sigma = 0.69, \tag{26}$$

$$g_{\sigma^*\Xi}/g_\sigma = 1.25. \tag{27}$$

We choose the temperature of the PNSs as $T = 15$ MeV [16].

As can be seen from Fig.1, TW99, DD-MEI and GM1 can give the masses of the PNSs PSR J0740+6620, PSR J0348+0432, PSR J1614-2230 and PSR J0737-3039A. Riley et al. [37] and Miller et al. [38] made accurate measurements of the mass and radius of NS PSR J0030+0451. Results of Riley et al. [37] are $M = 1.34^{+0.15}_{-0.16}\,M_\odot$ and $R = 12.71^{+1.14}_{-1.19}$ km, and results of Miller et al. [38] are $M = 1.44^{+0.15}_{-0.14}\,M_\odot$ and $R = 13.02^{+1.24}_{-1.06}$ km. We see that GM1 gives masses and radii that are closest to the results of [37,38]. Therefore, we next use GM1 to study the effect of the interaction between hyperons on the moment of inertia of the PNSs.

4. *Effect of the interaction between hyperons on the radius of the PNSs*. The radius of the PNS as a function of the mass calculated by nucleon

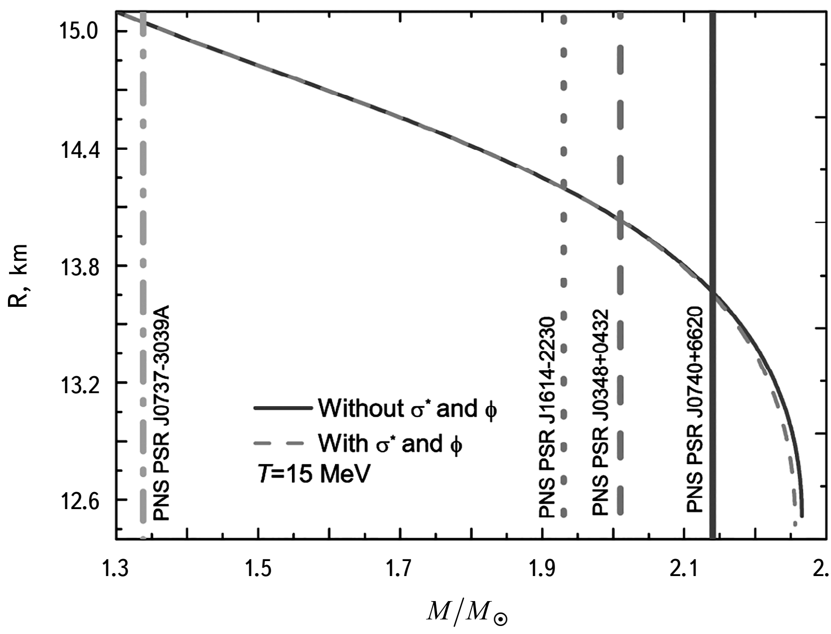

Fig.2. The radius of the PNS as a function of the mass calculated by nucleon coupling constant GM1. The four thick vertical lines represent the masses of the PNSs PSR J0740+6620, PSR J0348+0432, PSR J1614-2230 and PSR J0737-3039A, respectively.

coupling constant GM1 is shown in Fig.2. The nucleon coupling constant is chosen as GM1.

It can be seen that the radius R of the PNS decreases as the mass M increases. Given the interaction between hyperons, the mass M of the PNS decreases with respect to the same radius R.

Table 1

THE RESULTS OF THE CALCULATION OF THE RADIUS, CENTRAL ENERGY DENSITY, CENTRAL PRESSURE, AND MOMENT OF INERTIA

Parameter	R, km	ε_c, 10^{15} g cm^{-3}	p_c, 10^{35} dyne cm^{-2}	I, 10^{45} g cm^2
PNS6620 $M = 2.14 M_\odot$				
no σ^* and ϕ	13.663	1.124	2.577	2.347
with σ^* and ϕ	13.648	1.141	2.608	2.320
PNS0432 $M = 2.01 M_\odot$				
no σ^* and ϕ	14.035	0.931	1.820	2.443
with σ^* and ϕ	14.027	0.937	1.834	2.437
PNS2230 $M = 1.93 M_\odot$				
no σ^* and ϕ	14.199	0.856	1.533	2.425
with σ^* and ϕ	14.199	0.857	1.533	2.422
PNS3039A $M = 1.338 M_\odot$				
no σ^* and ϕ	15.05	0.563	0.553	1.671
with σ^* and ϕ	15.05	0.563	0.553	1.671

Under the constraints of the mass M of the corresponding PNS mentioned above, the radius of the PNS PSR J0740+6620 is reduced by about 0.1% from $R = 13.663$ km to $R = 13.648$ km considering the interaction between hyperons (see Table 1). The radius of the PNS PSR J0348+0432 decreases from $R = 14.035$ km to $R = 14.027$ km, which is about 0.06%. The radius of PNS PSR J1614-2230 is $R = 14.199$ km, while the radius of PNS PSR J1614-2230 is $R = 15.05$ km, both unchanged. We see that the larger the mass M of the PNS, the larger the reduction in the radius R of the PNS, taking into account the interaction between hyperons. For the less massive PNS, the hyperon interaction has little effect on the radius R. The influence of the interaction between hyperons on the radius of the PNS must lead to the influence on the moment of inertia.

5. *Effects of hyperon interactions on the energy density and pressure of the PNSs*. The energy density ε of the PNS as a function of the pressure p is shown in Fig.3.

We see that the energy density ε of the PNS increases as the pressure increases. Given the interactions between the hyperons, the energy density ε increases with respect to the same pressure p. Of course, the energy density ε doesn't go up very much.

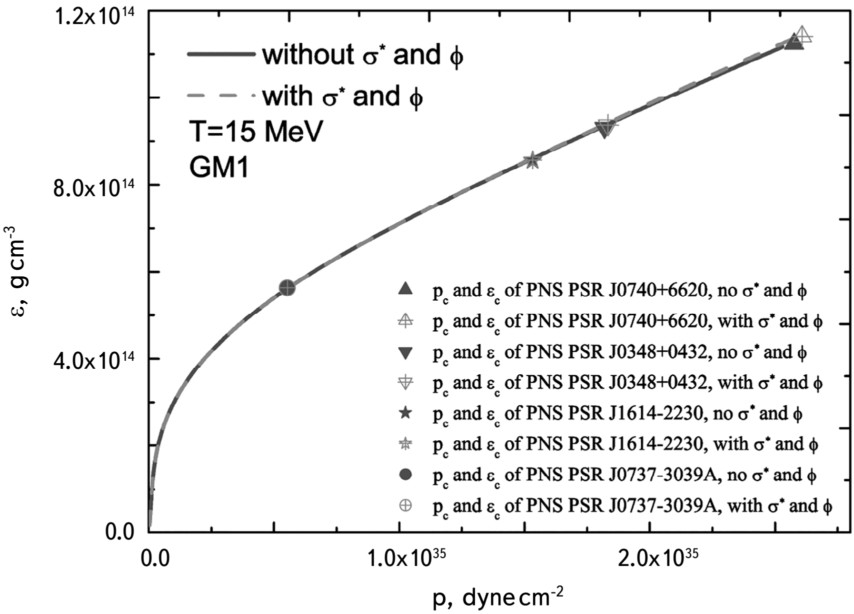

Fig.3. The energy density ε of the PNS as a function of the pressure p. The triangles, pentagons and dots in the figure represent the central energy density ε_c and central pressure p_c of the PNSs PSR J0740+6620, PSR J0348+0432, PSR J1614-2230 and PSR J0737-3039A, respectively. The solid symbols mean that the interaction between hyperons is not considered, and the hollow symbols mean that the interaction between hyperons is considered.

Under the constraint of the mass of the PNSs mentioned above, the central energy density of the PNS PSR J0740+6620 increases from $\varepsilon_c = 1.124 \cdot 10^{15}$ g cm^{-3} to $\varepsilon_c = 1.141 \cdot 10^{15}$ g cm^{-3} by about 1.5%, considering the interaction between hyperons. The central energy density of the PNS PSR J0348+0432 increases from $\varepsilon_c = 0.931 \cdot 10^{15}$ g.cm to $\varepsilon_c = 0.937 \cdot 10^{15}$ g cm^{-3}, which is about 0.6%. The central energy density of the PNS PSR J1614-2230 increases from $\varepsilon_c = 0.856 \cdot 10^{15}$ g cm^{-3} to $\varepsilon_c = 0.857 \cdot 10^{15}$ g cm^{-3}, increasing by about 0.1%. The central energy density of the PNS PSR J0777-3039A is $\varepsilon_c = 0.563 \cdot 10^{15}$ g cm^{-3}, which does not change. Similar results are found for the central pressure p_c of the PNSs. It can be seen that the larger the mass M of the PNS, the greater the influence of the interaction between hyperons on the central energy density ε_c and the central pressure p_c. When the mass M of the PNS is small, this effect can be ignored.

6. *The influence of the interaction between hyperons on the moment of inertia of the PNSs*. Fig.4 gives the moment of inertia I of the

PNS as a function of the central energy density ε_c.

As can be seen from Fig.4, the moment of inertia I of the PNS increases with the increase of the center energy density ε_c, and decreases with the increase of the center energy density ε_c after reaching a certain peak value. Taking into account the interaction between hyperons, the moment of inertia I of the PNS decreases with respect to the same central energy density ε_c.

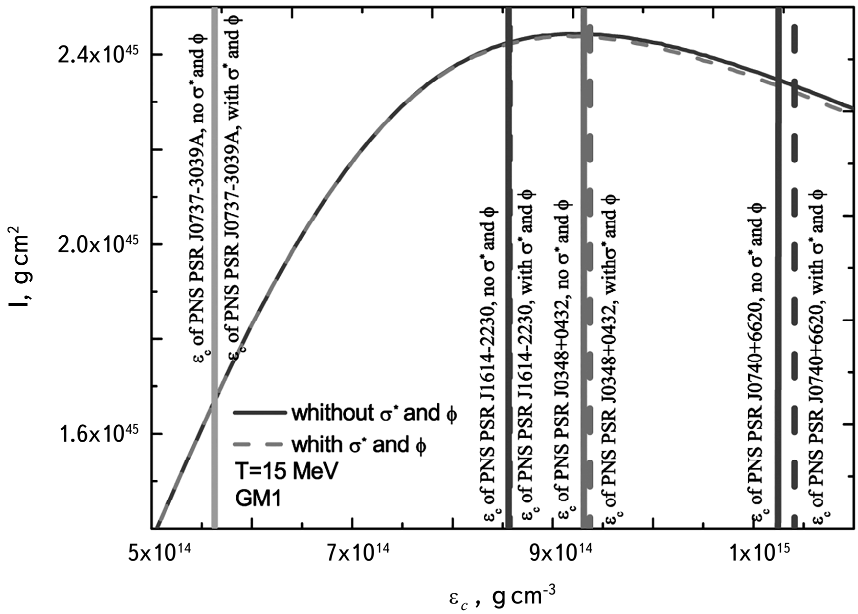

Fig.4. The moment of inertia I of the PNS as a function of the central energy density ε_c. The solid thick vertical lines represent the central energy density ε_c of the PNS when the interaction between hyperons is not considered, while the dashed thick vertical lines represent the central energy density ε_c of the PNS when the interaction between hyperons is considered.

We see from Table 1 and Fig.4, the moment of inertia I of the PNS PSR J0740+6620 is reduced from $I = 2.347 \cdot 10^{45}$ g cm^2 to $I = 2.320 \cdot 10^{45}$ g cm^2 by about 1.2% under the mass limit of the PNS mentioned above and considering the interaction between hyperons. The moment of inertia of the PNS PSR J0348+0432 decreases from $I = 2.443 \cdot 10^{45}$ g cm^2 to $I = 2.437 \cdot 10^{45}$ g cm^2, which is about 0.2%. The moment of inertia of the PNS PSR J1614-2230 decreases from $I = 2.425 \cdot 10^{45}$ g cm^2 to $I = 2.422 \cdot 10^{45}$ g cm^2, which is about 0.1%. The moment of inertia of the PNS PSR J0777-3039A is $I = 1.671 \cdot 10^{45}$ g cm^2 and does not change. So the larger the mass of the PNS, the larger the decrease in the moment of inertia considering the interaction between hyperons. When the mass of the PNS is small, the interaction between hyperons has little effect on the moment of inertia of the PNS.

The moment of inertia I of the PNS as a function of the radius R is shown in Fig.5. We see that the moment of inertia of the PNS increases as the radius increases, and after reaching a certain peak, decreases as the radius increases. Considering the interaction between hyperons, the moment of inertia of the PNS with respect to the same radius decreases, and the smaller the radius, the greater the decrease in moment of inertia.

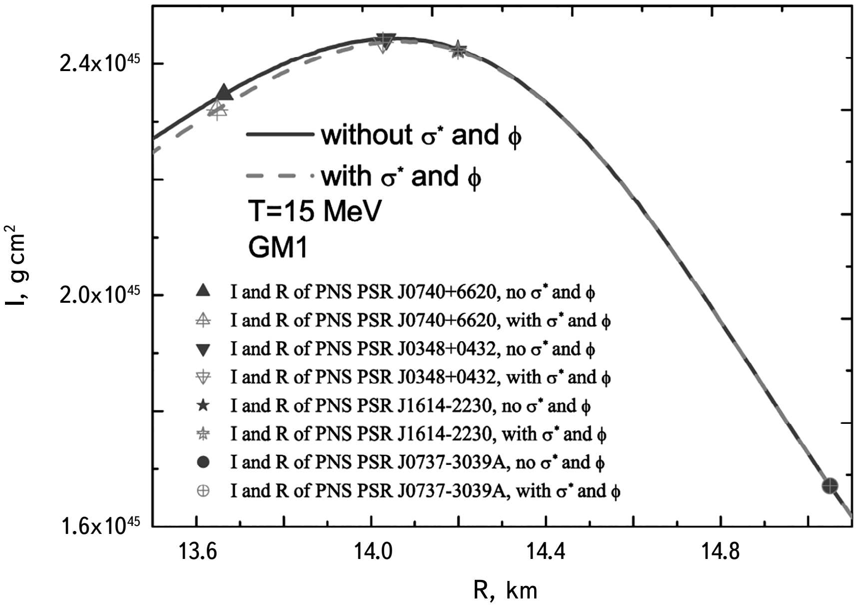

Fig.5. The moment of inertia I of the PNS as a function of the radius R. The triangles, pentagons and dots in the figure represent the moment of inertia I and radius R of the PNSs PSR J0740+6620, PSR J0348+0432, PSR J1614-2230 and PSR J0737-3039A, respectively. The solid symbols mean that the interaction between hyperons is not considered, and the hollow symbols mean that the interaction between hyperons is considered.

The moment of inertia I of the PNS as a function of the mass M is given in Fig.6. We see that the moment of inertia of the PNS increases with the increase of the mass, and after reaching a certain peak, decreases with increase of the mass. Taking into account the interaction between hyperons, the moment of inertia of the PNS with respect to the same mass decreases, and the greater the mass, the greater the decrease in the moment of inertia.

7. *Summary*. In this paper, the effects of the interaction between hyperons on the moment of inertia of the PNSs PSR J0740+6620, PSR J0348+0432, PSR J1614-2230 and PSR J0737-3039A are studied by means of RMF theory. The nucleon coupling parameter is chosen as GM1, and the temperature of the PNS is set as $T=15$ MeV.

We see that the mass M of the PNS decreases with respect to the same radius

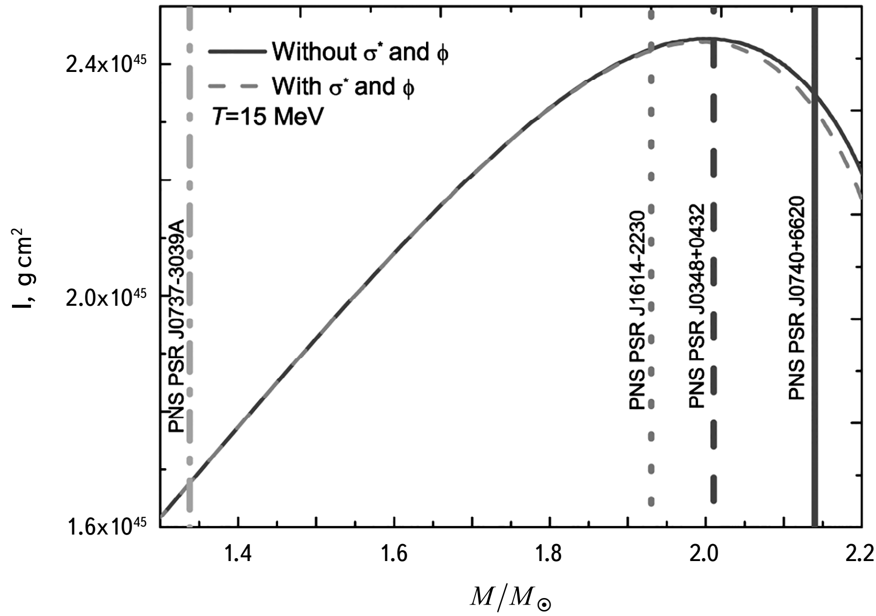

Fig.6. The moment of inertia I of the PNS as a function of the mass M. The four thick vertical lines represent the masses of the PNSs PSR J0740+6620, PSR J0348+0432, PSR J1614-2230 and PSR J0737-3039A, respectively.

R as the interaction between hyperons is considered. Under the constraints of the mass M of the corresponding PNS, the larger the mass M of the PNS, the larger the reduction in the radius R of the PNS, taking into account the interaction between hyperons. For the less massive PNS, the hyperon interaction has little effect on the radius R.

Under the constraint of the mass of the PNSs, the larger the mass M of the PNS, the greater the influence of the interaction between hyperons on the central energy density ε_c and the central pressure p_c. When the mass M of the PNS is small, this effect can be ignored.

Taking into account the interaction between hyperons, the moment of inertia I of the PNS decreases with respect to the same central energy density ε_c. We also see that the larger the mass of the PNS, the larger the decrease in the moment of inertia considering the interaction between hyperons. When the mass of the PNS is small, the interaction between hyperons has little effect on the moment of inertia of the PNS.

Our results show that the interaction between hyperons has a strong influence on the properties of the larger mass PNS, but a small influence on the properties of the smaller mass PNS.

In our calculation, in addition to the mean-field approximation, we also use the sea-free approximation, that is, we do not consider the effect of antiparticles. In fact, especially in finite temperature NS matter, antiparticles excited from the sea should be considered. This will be an area that we will continue to investigate in the future.

In addition, the simplest RMF model with constant baryon-meson couplings is used in our calculations and the so-called rearrangement self-energy is not taken into account. But it is necessary to include properly the "rearrangement" contributions to show that energy-momentum conservation [25]. Therefore, the influence of the rearrangement self-energy on the NS/PNS matter should be considered in the next calculations.

This work was supported by the Natural Science Foundation of China (Grant No. 11447003).

School of Sciences, Southwest Petroleum University, China,
e-mail: zhaopioneer.student@sina.com

ВЛИЯНИЕ ВЗАИМОДЕЙСТВИЯ ГИПЕРОНОВ НА МОМЕНТ ИНЕРЦИИ ПРОТОНЕЙТРОННЫХ ЗВЕЗД

СИАНЬ-ФЭН ЧЖАО

В рамках релятивистской теории среднего поля исследовано влияние взаимодействия гиперонов на момент инерции протонейтронных звезд (ПНЗ) PSR J0740+6620, PSR J0348+0432, PSR J1614-2230 и PSR J0737-3039A. При учете взаимодействия между гиперонами: а) при одинаковом радиусе R масса ПНЗ уменьшается, б) при одинаковом давлении p плотность энергии увеличивается, в) при одинаковой центральной плотности ε_c момент инерции I ПНЗ уменьшается. При ограничении массы ПНЗ, в результате взаимодействия между гиперонами, чем больше масса ПНЗ, тем больше уменьшаются радиус и момент инерции ПНЗ, а плотность энергии и давление увеличиваются. Для менее массивных ПНЗ эффект может быть незначительным.

Ключевые слова: *гиперон:релятивистская теория среднего поля:нейтронная звезда*

REFERENCES

1. *X.L.Mu*, *H.Y.Jia*, *X.Zhou et al.*, Astrophys. J., **846**, 140, 2017.
2. *Z.L.Deng*, *X.D.Li*, *Z.F.Gao et al.*, Astrophys. J., **909**, 174, 2021.
3. *W.B.Ding*, *M.D.Cai*, *A.H.Chan et al.*, Int. J. Mod. Phys. A, **37**, 2250034, 2022.
4. *Y.X.Li*, H.Y.Chen, *D.H.Wen et al.*, Eur. Phys. J. A, **57**, 31, 2021.
5. *J.B.Hartle*, Astrophys. J., **150**, 1005, 1967.
6. *J.B.Hartle*, *K.S.Thorne*, Astrophys. J., **153**, 807, 1968.
7. *A.G.Lyne*, *M.Burgay*, *M.Kramer et al.*, Science, **303**, 1153, 2004.
8. *S.E.Thorsett*, *D.Chakrabarty*, Astrophys. J., **512**, 288, 1999.
9. *M.Bailes*, *S.M.Ord*, *H.S.Knight et al.*, Astrophys. J., **595**, L49, 2003.
10. *I.A.Morrison*, *T.W.Baumgarte*, *S.L.Shapiro et al.*, Astrophys. J., **617**, L135, 2004.
11. *M.Kramer*, *I.H.Stairs*, *R.N.Manchester et al.*, Science, **314**, 97, 2006.
12. *P.B.Demorest*, *T.Pennucci*, *S.M.Ransom et al.*, Nature, **467**, 1081, 2010.
13. *E.Fonseca*, *T.T.Pennucci*, *J.A.Ellis et al.*, Astrophys. J., **832**, 167, 2016.
14. *J.Antoniadis*, *P.C.C.Freire*, *N.Wex et al.*, Science, **340**, 448, 2013.
15. *H.T.Cromartie*, *E.Fonseca*, *S.M.Ransom et al.*, Nature Astron., **4**, 72, 2020.
16. *A.Burrows*, *J.M.Lattier*, Astrophys. J., **307**, 178, 1986.
17. *J.Schaffner*, *C.B.Dover*, *A.Gal*, Ann. Phys., **235**, 35, 1994.
18. *S.G.Zhou*, Phys. Scr., **91**, 063008, 2016.
19. *N.K.Glendenning*, Compact Stars: Nuclear Physics, Particle Physics, and General Relativity, Springer-Verlag, New York, Inc, 1997.
20. *N.K.Glendenning*, Phys. Lett. B, **185**, 275, 1987.
21. *N.K.Glendenning*, Nucl. Phys. A, **469**, 600, 1987.
22. *A.Sedrakian*, *A.Harutyunyan*, Universe, **7**, 380, 2021, arXiv:2109.01919.
23. *R.C.Tolman*, Phys. Rev., **55**, 364, 1939.
24. *J.R.Oppenheimer*, *G.M.Volkoff*, Phys. Rev., **55**, 374, 1939.
25. *S.Typel*, *H.H.Wolter*, Nucl. Phys. A, **656**, 331, 1999
26. *T.Laura*, *C.Mario*, *R.Angels*, Publ. Astron. Soc. Aust., **34**, e065, 2017
27. *B.G.Todd-Rutel*, *J.Piekarewicz*, Phys. Rev. Lett., **95**, 122501, 2005.
28. *N.K.Glendenning*, Astrophys. J., **293**, 470, 1985.
29. *N.K.Glendenning*, *S.A.Moszkowski*, Phys. Rev. Lett., **67**, 2414, 1991.
30. *J.Schaffner*, *I.N.Mishustin*, Phys. Rev. C, **53**, 1416, 1996.
31. *J.Schaffner-Bielich*, *A.Gal*, Phys. Rev. C, **62**, 034311, 2000.
32. *X.F.Zhao*, Int. J. Theor. Phys., **58**, 1060, 2019
33. *S.Weissenborn*, *D.Chatterjee*, *J.Schaffner-Bielich*, Nucl. Phys. A, **881**, 62, 2012.
34. *A.Gal*, *E.V.Hungerford*, *D.J.Millener*, Rev. Mod. Phys., **88**, 035004, 2016.
35. *C.J.Batty*, *E.Friedman*, *A.Gal*, Phys. Rep., **287**, 385, 1997.
36. *T.Harada*, *Y.Hirabayashi*, *A.Umeya*, Phys. Lett. B, **690**, 363, 2010.
37. *T.E.Riley*, *A.L.Watts*, *S.Bogdanov et al.*, Astrophys. J. Lett., **887**, L21, 2019.
38. *M.C.Miller*, *F.K.Lamb*, *A.J.Dittmann et al.*, Astrophys. J. Lett., **887**, L24, 2019.